Evaluating the Effect of Z-pinning Parameters on the Mechanical Strength and Toughness of Printed Polymer Composite Structures

Brenin Bales[1], Tyler Smith[2], Seokpum Kim[2], Vlastimil Kunc[1,2], Chad Duty[1,2]

[1]University of Tennessee
Knoxville, TN

[2]Manufacturing Demonstration Facility
Oak Ridge National Laboratory
Oak Ridge, TN

Abstract

Traditional Fused Filament Fabrication methods create a mechanically anisotropic structure that is stronger in the deposition plane than across successive layers. A recently developed pinning process deposits continuous pins in the structure that are orientated in the build direction across multiple layers. Initial studies of this technique have demonstrated the ability to increase inter-layer strength and toughness. The current study evaluated various z-pinning parameters for carbon fiber reinforced polylactic acid (CF-PLA) structures, including infill percentage, pin length, and deposition pattern. Each of these was found to affect the ability of the z-pin to mechanically bond with the existing lattice structure and had a resulting impact on the mechanical strength and toughness. Initial studies showed an increase in ultimate tensile strength in the Z-axis of around 3.5x. Upon expanding the pinning settings, further studies showed increases of over 35% from the X and Z axis ultimate tensile strength and improved mechanically isotropic behavior.

Introduction

Fused Filament Fabrication (FFF) is a method of AM in which consecutive layers of material are deposited onto each other in one direction, typically parallel to the build platform. The 3D printed structures will be built in the Z-Axis (build direction). Traditional FFF methods create mechanically anisotropic structures due to their consecutive layer printing. When printing layers of material, the strength of the structure is strongest when the beads of material are aligned (0^{o}) to one another in the load direction (X-Y Plane), as a byproduct, this creates a very anisotropic structure. Compared to when the beads of material are normal (90^{o}) to each other in successive layers, strength falls by 40-85%, but the structure behaves as a quasi-isotropic structure **[1–3]**.

When comparing the deposition plane (**X/Y)** to successive layers in the build direction **(Z)** the anisotropic behavior of the print leads to a drop in strength. This drop in strength can range from 25-90%. Looking at **Table 1**, the drop in ultimate tensile strength between ABS materials ranges from 25-79% across both large (BAAM/LSAM) and small (FFF) area additive manufacturing platforms **[4–10]**. The material of choice for this project is the 15% CF-PLA,

which when comparing the ultimate tensile strength across the X and Z axis, shows a 34% drop in strength**[10]**.

Material	Platform	UTS_x	UTS_z	Reduction	Reference
ABS					
ABS	FFF	31 MPa	6.6 MPa	79%	[4]
ABS	FFF	29 MPa	14 MPa	52%	[5]
ABS	FFF	34 MPa	18 MPa	47%	[6]
ABS	BAAM*	36 MPa	27 MPa	25%	[7]
ABS	LSAM**	22 MPa	11 MPa	50%	[8]
5% Jute-ABS	FFF	26 MPa	13 MPa	50%	[5]
5% Jute-ABS	FFF	24 MPa	8.6 MPa	64%	[6]
13% GF-ABS/LLDPE^	FFF	39 kg	1.2 kg	97%	[9]
18% GF-ABS/LLDPE^	FFF	59 kg	11 kg	81%	[9]
20% GF-ABS	BAAM*	67 MPa	13 MPa	81%	[7]
20% CF-ABS	BAAM*	67 MPa	8.2 MPa	88%	[7]
PLA					
PLA	FFF	56 MPa	24 MPa	57%	[4]
PLA	FFF	55 MPa	37 MPa	33%	[10]
15% CF-PLA	FFF	53 MPa	35 MPa	34%	[10]

Table 1: Mechanical Anisotropy of Extrusion-Based Printed Samples [11]

Researchers have come up with many different proposed solutions to alleviate the drop in strength across layers. Initial work on increasing the inter-layer bond strength has focused on increasing the inter-diffusion of polymer chains across the interface **[12]**. To increase the inter-layer bond strength it is critical to keep the build temperature to at least the glass transition temperature of the material **[12–14]**.In order to do this, some researchers investigated adding another heat source during the deposition process. A Montana State University research team investigated increasing the interface temperature by introducing a stream of hot air **[15]**. This method was not effective due to the additional air flow effecting the geometry of the build and not improving the strength of the material. Alternatively, work done at Arizona State University increased the flexural strength by 50% in an ABS (0.03% Carbon Black ABS) by adding a laser-based pre-deposition method to increase the temperature of the deposition surface **[16,17]**. Oak Ridge National lab also investigated additional heating methods by mounting infrared lamps onto the BAAM printing head, where after preheating, the fracture energy of 20% CF-ABS**[18]** had doubled. This research further explores a novel printing approach, called z-pinning, that was first presented at SFF in 2017 **[19,20]**.

Z-Pinning

The Z-pinning process was developed to increase z-axis strength and reduce mechanical anisotropy. The Z-pinning process in composite AM manufacturing aims to achieve similar goals to the Z-pinning processes already being used in the traditional composites manufacturing industry to eliminate delamination and improve through-thickness properties [21,22]. The z-pinning process for FFF relies on using the same material throughout the build. The current process uses intentionally created aligned gaps over successive layers **(see Fig. 1)** to create a void where the pin is dropped through multiple layers. The pinning process starts by dropping in the pins through a set amount (set using the pin parameters) of layers **(Fig. 1a).** The next two steps of the process **(Fig. 1b and 1c)** show the pin being deposited across multiple layers. As the pins are deposited on top of one another, a "seam line" is created between the two consecutive pins. This seam line is a potential source of a failure. It is important to note that the pins are staggered as to avoid creating a seamline, which can lead to defects in the print **(Fig. 1d)**. Next, after laying down another set of layers, the nozzle will be positioned over the already deposited pin **(Fig. 1e and 1f)** and stack the pins on top of one another. The z-pinning method's effectiveness is determined by how well the pins mechanically interlock with the surrounding layered structure[23] and how well the materials bond to one another. This is determined by the various pin parameters that determine the overall shape and size of the pin.

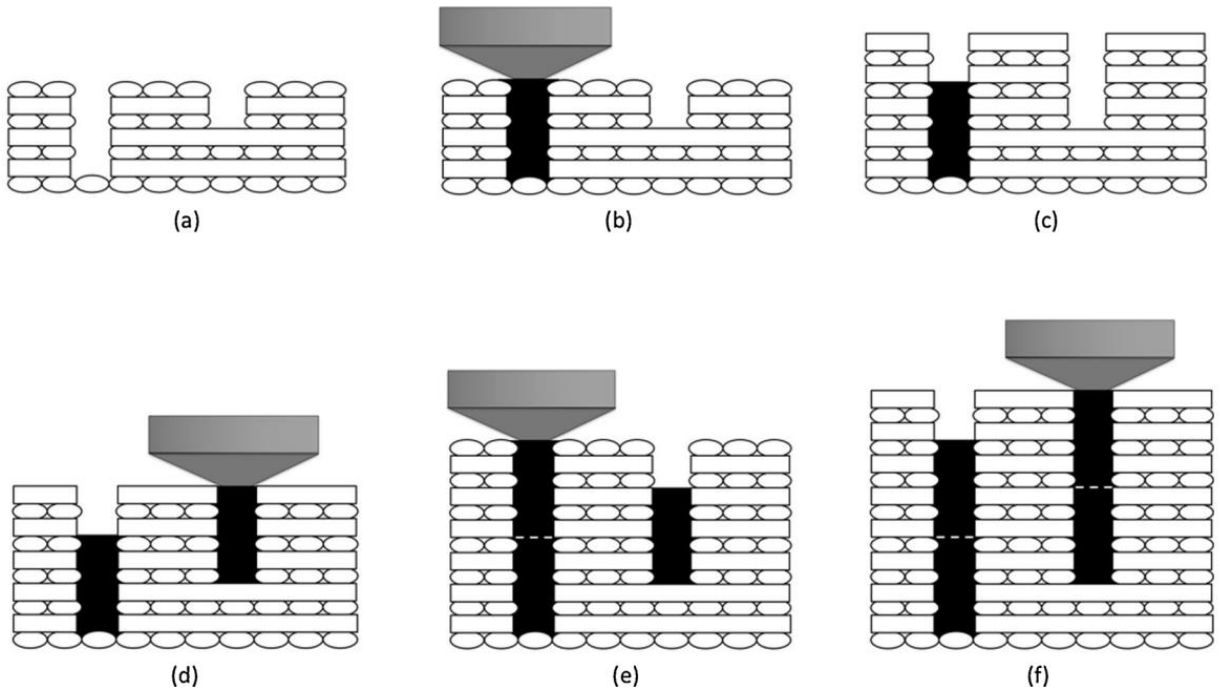

Figure 1: The z-pinning process[11]

The pin parameters are the pin width, pin length, deposition pattern (seam offset), and the infill percentage. The pins themselves are designed as a prismatic pin with a square cross section with a length that spans a specific number of layers. The pin width defines how wide the pin is, ranging from 1.5mm to 3mm. Pin length determines how many layers the pin will be deposited across, either 8, 12, or 20 layers. The deposition pattern of the pin affects where the seams will line up with one another. This is otherwise known as the seam offset. The seam offset is set at

half of the pin length of the pin. This means that the pins will have a staggered seam pattern so to not create an obvious fracture line **(See Fig. 2)**. The final pin parameter is the infill percentage. The infill percentage is defined as the amount of material that is deposited into the pin gap compared to the theoretical volume of the gap itself. how much material is deposited into the void. The current infill percentages being tested are 80%, 100%, and finally an "overflow" at 120%. The ability to "overflow" the pin gap is due to the nature of the rectilinear grid structure part, meaning that the material is laid down in alternating X/Y deposition paths (See **Fig. 3).**

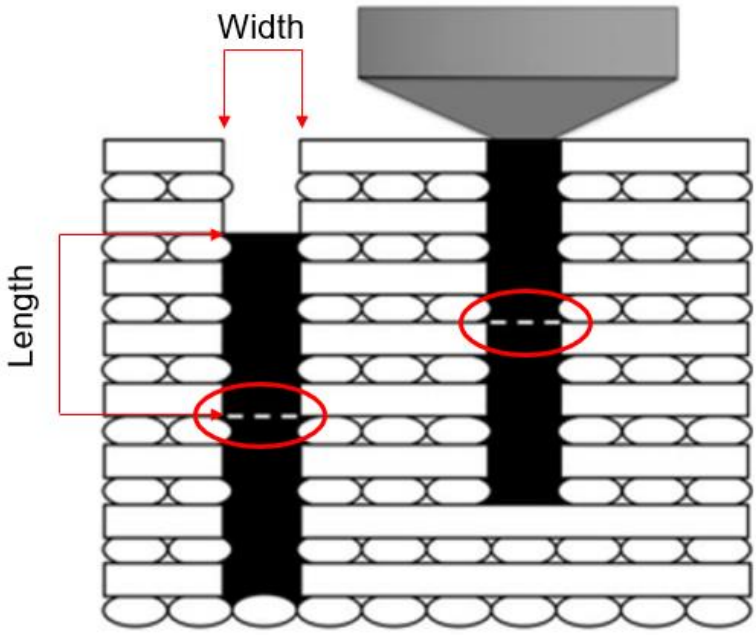

Figure 2: Pin Parameters [4]

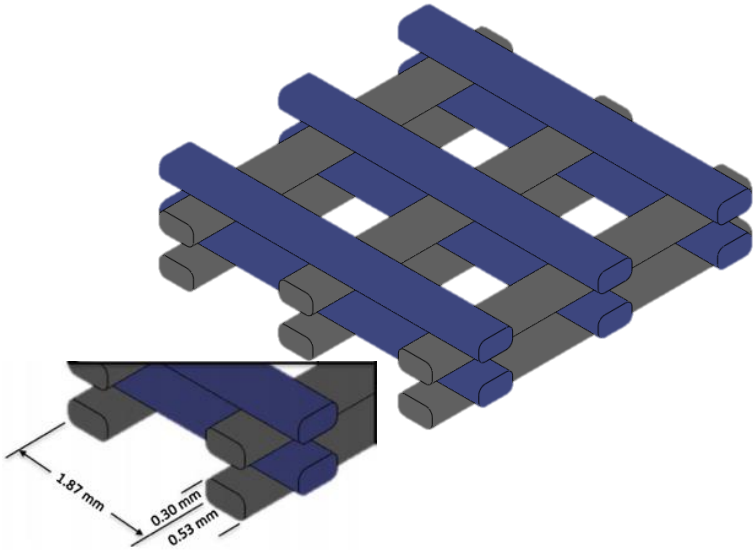

Figure 3: Rectilinear Grid [11]

Initial studies in z-pinning showed promising results in both improving the z-axis ultimate tensile strength (UTS_z) and leading towards quasi-isotropic data in some of the data sets. The pin parameters used for the first round of research consisted of a pin length of 4-8, meaning the pins were 8 layers long and staggered at 4 layers. While the pin width was held at 3W, which sets the width to be 1.5mm. The infill percentages varied from 80%, 100%, 120% with additional data sets at a solid infill (standard rectilinear grid) and 0% infill (no pins in the voids).

Figure 4 shows the relationship between the ultimate tensile strength of the X-axis (UTS_x) and Z-axis (UTS_z) [11]. The pin parameter that showed the greatest ultimate tensile strength was the solid sample set. The solid sample showed a 33% degree of anisotropy between the X and Z axis. Looking at the pinned samples, from 0%-120% samples increased in strength and decreased in anisotropy. The 120% infill samples showed an average UTS_z over 3.5x greater than the 0% infills samples **(See Fig 4)**. Additionally, the 120% samples showed the lowest anisotropy. Additionally, the goals of the next phase of research is to systematically investigate what effects different pin parameters have on the mechanical strength and isotropy of printed parts.

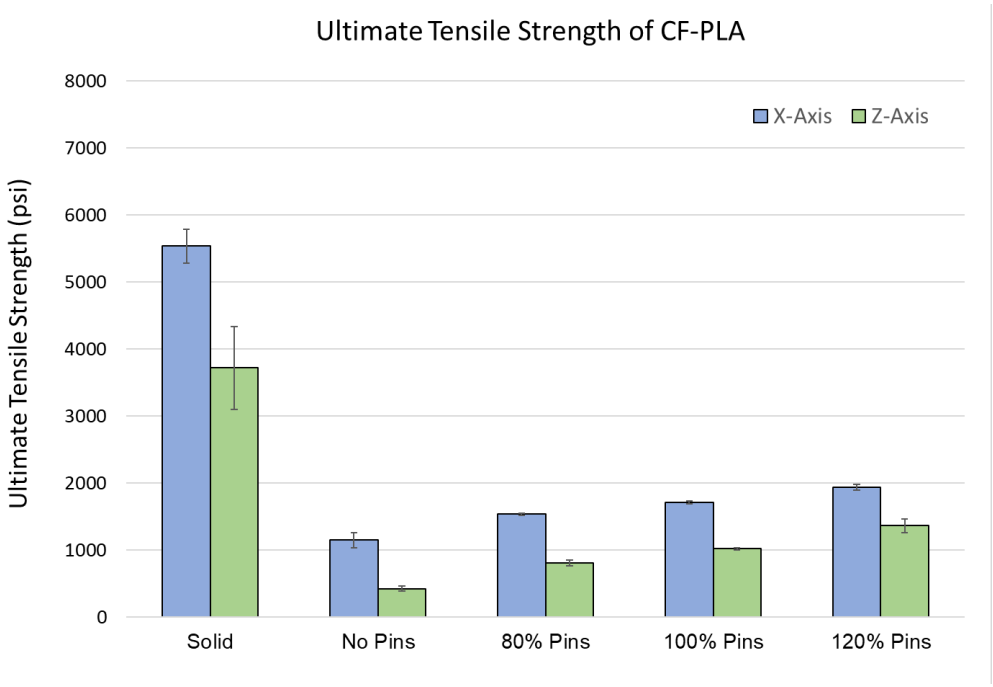

Figure 4: Ultimate Tensile Strength of CF-PLA [11]

Experimental Methods

The printed samples were walls measuring 12.7cm x 1.27cm x 12.7cm **(Fig. 5)** Printed using a MakerGear M2 Desktop printer. The material used was 1.75mm diameter CarbonX from 3DXTech. The CarbonX material is a carbon fiber reinforced PLA (CF-PLA) [24] containing a 15% weight carbon fiber reinforced PLA (CF-PLA) [25]. Printing took place at a nozzle temperature of 225ºC and a bed temperature of 65ºC. This slight increase over the recommended

temperatures of 220ºC (extruder) and 60ºC (bed) was selected for the additional benefits of increased bonding to the print bed. The software used to generate the g-code was Matlab and was programmed to create a rectilinear grid of alternating X and Y axis deposition paths. The rectilinear grid has a 35% infill pattern with preset voids to insert the pins. The rectilinear grid was deposited with a bead dimension of 0.53 mm wide 0.30mm thick. To create the 35% infill, the beads were spaced apart by 1.87 mm **(Fig. 3)**.

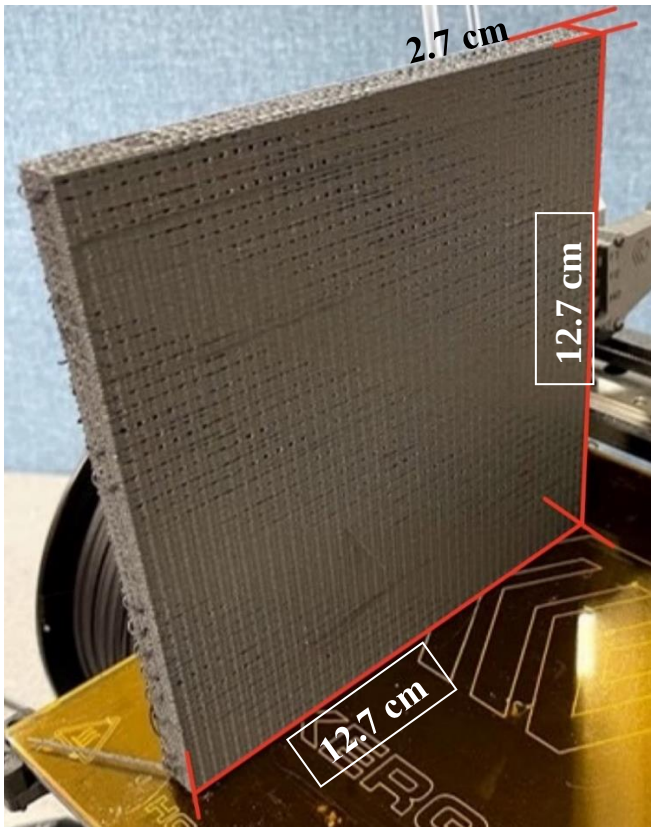

Figure 5: Print Sample with Dimensions

During the printing process 4 walls were printed for each pin parameter. This is necessary because each wall will yield three tensile samples (for a total of 6 samples), which allows us to have enough samples for a standard deviation, per ASTM D638 **[26]** . The walls are then milled to less than 9mm in thickness, which allows the samples to fit inside of the grips of the tensile tester. After milling, the walls were waterjet cut into 3 tensile test specimens per wall. Two of the walls were cut in with perpendicular to the build path (Z-samples), while the other two walls are cut parallel to the build path (X-samples) **(Fig. 6)**. The sample geometry was a modified Type 4 tensile specimen per ASTM D638 **(Fig. 7) [26]**. The tensile test specimens were a modified geometry due to the need for a sufficient number of pins across the gage area. If there are not enough pins across the gage area, then the pins will have an insufficient effect on the material properties of the samples. Before testing the samples are dried in an oven for at least 8 hours at 50ºC. Mechanical testing is conducted using an MTS servo-hydraulic tensile tester equipped with a 110kn load cell with a strain rate of 3 mm/min.

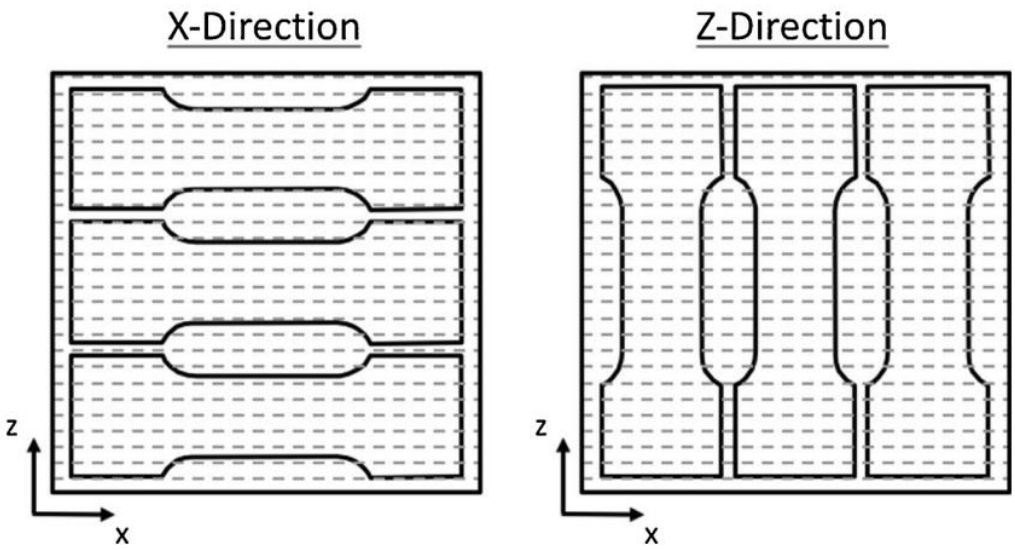

Fig 6: Orientation of Tensile Samples [11]

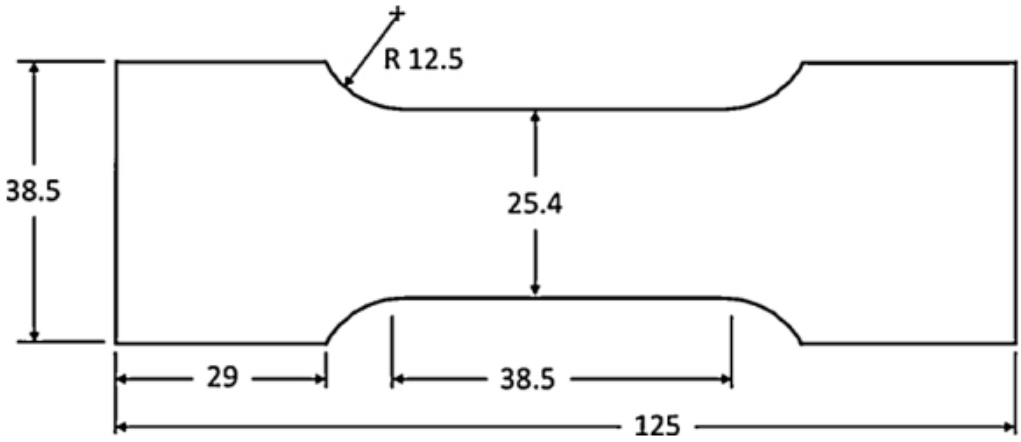

Fig 7: Modified Type 4 Tensile Sample, dimensions in mm [11]

This stage of the z-pinning involved expanding the pin parameter set to discover if any alterations to the pins would give them an advantage in ultimate tensile strength. Additionally, if any of the new pin parameters would lead to a more isotropic data set. The first set of pin parameters that were expanded upon were more 80% infill pins, this is the focus for this study. The set of parameters that were first identified were the 3W (1.5mm) pin width, and the pin lengths of 4-8 and 6-12. After the 3W set, 4W (2mm) and 6W (3mm) were also printed and tested. Both of those samples were printed at the 6-12 pin length.

Results and Discussions

Tensile data will be analyzed in using two methods. First, the strength ratio, which is a percent change between the between the ultimate tensile data of the 0% infill sample **(See Fig. 4)** and the ultimate tensile strength of the selected sample (See Eq. 1). The strength ratio will allow a direct comparison between how the z-pinning process (and the different parameters) will affect

a unpinned print, specifically with a pin width of 3W[11]. The other metric is a calculation of the anisotropy ratio. The anisotropic ratio is the ratio of UTS_z to UTS_x for a given sample. This ratio will demonstrate how the different pin parameters effect the individual tensile strengths and how they relate to one another.

$$\left(\frac{UTS_{0\%} - UTS_{80\%}}{UTS_{0\%}}\right) x\ 100$$

Equation 1: Strength Ratio Comparison

Tensile tests results shown in **Figure 8** for all 80% pin widths. The tensile sample with a pin width of 3W, and a pin length of 4-8 demonstrated a 53.4% decrease in strength when comparing UTS_x to UTS_z. The final tensile sample at 3W had a pin length of 6-12. The pin length corresponded to a 63.7% decrease in strength (**Fig. 8)**. The final two sample sets at 80% were a 4W/6-12 and a 6W/4-8. The 4W/6-12 sample was chosen as the "middle ground" in the parameter matrix (**Fig 8)**, which would in theory yield a combination of the best tensile strength and easiest print process. Looking at **Figure 8**, the 4W/6-12 sample demonstrated a 52.4% decrease in Ultimate tensile strength, the second lowest. The 6W/4-8 sample was chosen due to the difficulties involved with printing 6W sample sets, it also demonstrated a 48% decrease in strength, the lowest of all the tensile specimens.

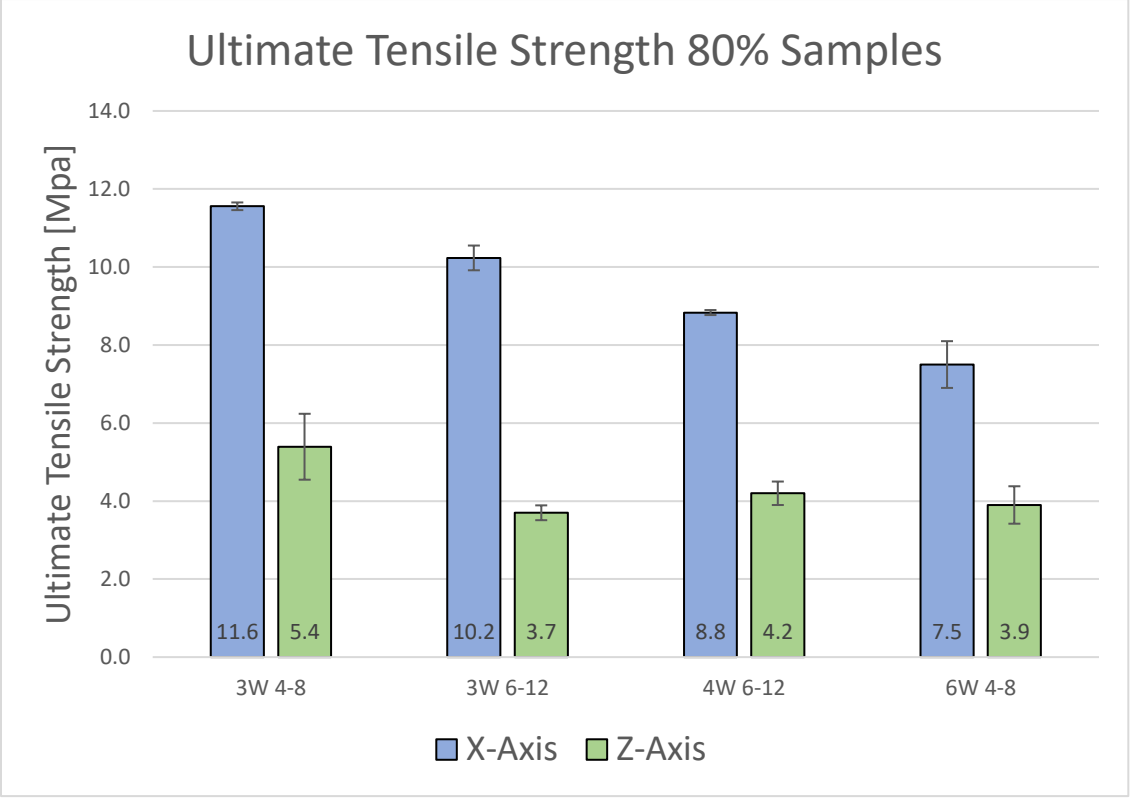

Figure 8: Ultimate Tensile Strength of 80% Infill Samples

Table 2 compared the anisotropy ratios of tensile samples according to their pin width and length. The anisotropy ratio is the UTS_z divided by UTS_x. For the 3W pin widths, the 4-8 sample had an anisotropy ratio of 0.47. While the 3W/6-12 pin length had an anisotropy ratio of 0.36, the lowest of the tensile samples. The 4W/6-12 sample yielded the second highest at 0.48, which combined with the second lowest drop in UTS **(Fig 8)**, validated the testing choice. The 6W/4-8 sample showed the highest anisotropy ratio at 0.52, but only achieved this by decreasing the UTS_x when compared to an unpinned 3W sample (**Table 3)**.

80% Infill Z/X	**3W**	**4W**	**6W**
4-8	5.4/11.6 = 0.47		3.9/7.5 = 0.52
6-12	3.7/10.2 = 0.36	4.2/8.8 = 0.48	
10-20			

Table 2: Anisotropic Ratio of Ultimate Tensile Strength

The last analysis method used was the strength ratio, described in **Equation 1**. The strength ratio compared the ultimate tensile strength of the pinned samples, to an unpinned block at 3W pin width, these results are shown in **Table 3**. The first samples at a 3W/3-8 showed a 46% increase in UTS_z and an increase of 85% for UTS_x **(Table 3).** The 6-12 pin length sample for 3W only increased the UTS_x by 29% and UTS_z by 27%. The last two sample sets shown in **Table 3** were the 4W/6-12 sample and 6W/4-8. The strength ratio of the 4W/6-12 sample, demonstrated only a 11% increase in the UTS_x, but improved the UTS_z by 44% **(Table 3)**. When comparing the strength ratios of the 6W/4-8 to the unpinned sample at 3W the UTS_x decreased by 5.4%. While UTS_z increased by 33.6% **(Table 3)**.

Strength Ratio	**3W 4-8**	**3W 6-12**	**4W 6-12**	**6W 4-8**
UTS_x	46%	29%	11%	-5.4%
UTS_y	85%	27%	44%	33.6%

Table 3: Strength Ratio of Ultimate Tensile Strength

Defects

Throughout the experiment one of the discoveries was how each pin parameter can affect the printing process of the wall. For a successful pin creation, the nozzle must deposit the material into the pin void **(See Fig. 2b)** without coming into major contact with the side walls early. If the pins contact the walls to early, voids will be created **(See Fig. 9)** [27]. These voids lead to two major sources of error. First, the voids lead to obvious fracture defects that effect the behavior of the sample during the testing process. Additionally, the voids cause the material to pile up before they fall the full length of the pin cavity. This will cause “overflow” errors. Overflow errors result in excess material building up on the printing surface of the build, which then runs into the nozzle during the printing process. Once a significant number of layers has been deposited, the build will sometimes times “step” and fall over.

Additionally, analysis of where the defects occurred highlighted how time consuming and difficult printing at a width of 6W was. Going forward, the scope of 6W testing will be reduced to focus more on pin parameters that are more practical to investigate.

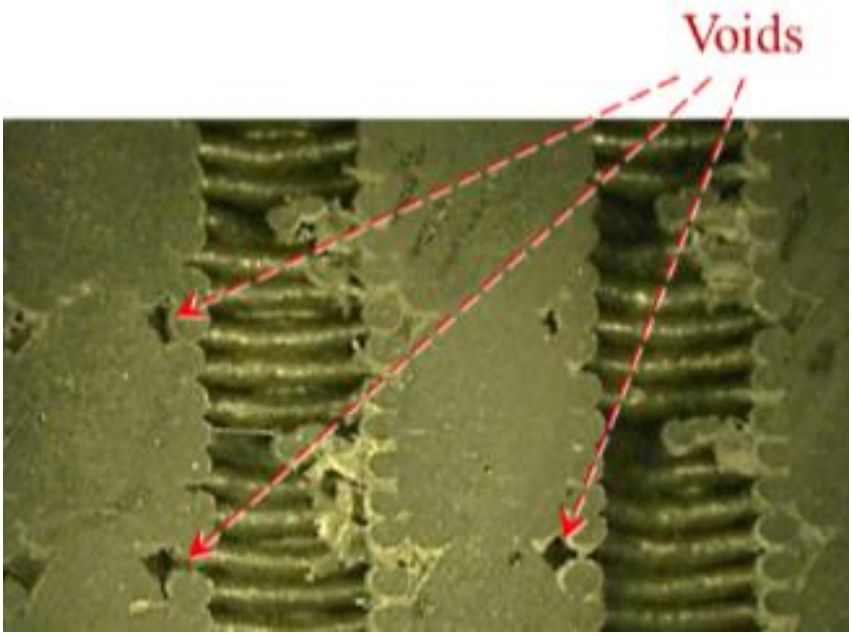

Fig 9: Voids in Pin Printing[27]

Conclusions and Future Work

Research into z-pinning is still on going, the initial round of research conducted established that the z-pinning method is effective. Prior work [11] concluded that introducing pins into a 35% infill structure was able to increase the toughness and ultimate tensile strength in the z-axis by over 3.5x. Upon expanding the scope of the research to explore a wider range of pin parameters, the effect of the change in pin parameters can be seen directly through the strength ratios of each tensile sample set. The 3W/4-8 tensile sample demonstrated the greatest increase in tensile strength in both axis by 45% when compared to the unpinned sample **(See Fig. 4)**. While pin lengths of 6-12 at both the 3W and 4W pin width only showed modest increases in ultimate tensile strength, 26-29% (3W) and 11-44% (4W). The 6W pin width with a 6-12 pin length proved to be the least advantageous, with a decrease in UTS_x by 5.4%, with the second lowest increase in UTS_z of 33.6%. Looking at the anisotropy ratios **(Table 1)**, the performance of the 6W/4-8/80% sample showed that while the UTS_x decreased, the increased UTS in the Z-axis yielded the best anistropic ratio of 0.52. It is important to note that while the 6W tensile sample led to the best anisotropic ratio, it only achieved this by reducing its UTS_x. As more pin parameters are investigated, this drop in strength, and how it affects the anisotropic ratio will be taken into consideration. Further expansion of the pin parameters into the 100% infill range is planned, to identify the best isotropic ratio and mechanical performance. Additionally, more tests to round out the 80% infill pattern are being conducted, particularly in the 10-20 pin length.

Acknowledgements

Research sponsored by the U.S. Department of Energy, Office of Energy Efficiency and Renewable Energy, Advanced Manufacturing Office, under contract DE-AC05-00OR22725 with UT-Battelle, LLC. This work was supported in part by Oak Ridge Institute for Science and Education through the Higher Education Research Experiences Program (HERE). Research was also sponsored by the U.S. Army Combat Capabilities Development Command Aviation & Missile Center.

References

[1] A. Bellini, S. Güçeri, Mechanical characterization of parts fabricated using fused deposition modeling, Rapid Prototyp. J. 9 (2003) 252–264. https://doi.org/10.1108/13552540310489631.

[2] S. Ahn, M. Montero, D. Odell, S. Roundy, P.K. Wright, Anisotropic material properties of fused deposition modeling ABS, Rapid Prototyp. J. 8 (2002) 248–257. https://doi.org/10.1108/13552540210441166.

[3] O.S. Es-Said, J. Foyos, R. Noorani, M. Mendelson, R. Marloth, B.A. Pregger, Effect of Layer Orientation on Mechanical Properties of Rapid Prototyped Samples, Mater. Manuf. Process. 15 (2000) 107–122. https://doi.org/10.1080/10426910008912976.

[4] S. Shaffer, K. Yang, J. Vargas, M.A. Di Prima, W. Voit, On reducing anisotropy in 3D printed polymers via ionizing radiation, Polymer. 55 (2014) 5969–5979. https://doi.org/10.1016/j.polymer.2014.07.054.

[5] A.R. Torrado Perez, D.A. Roberson, R.B. Wicker, Fracture Surface Analysis of 3D-Printed Tensile Specimens of Novel ABS-Based Materials, J. Fail. Anal. Prev. 14 (2014) 343–353. https://doi.org/10.1007/s11668-014-9803-9.

[6] A.R. Torrado, C.M. Shemelya, J.D. English, Y. Lin, R.B. Wicker, D.A. Roberson, Characterizing the effect of additives to ABS on the mechanical property anisotropy of specimens fabricated by material extrusion 3D printing, Addit. Manuf. 6 (2015) 16–29. https://doi.org/10.1016/j.addma.2015.02.001.

[7] C.E. Duty, V. Kunc, B. Compton, B. Post, D. Erdman, R. Smith, R. Lind, P. Lloyd, L. Love, Structure and mechanical behavior of Big Area Additive Manufacturing (BAAM) materials, Rapid Prototyp. J. 23 (2017) 181–189. https://doi.org/10.1108/RPJ-12-2015-0183.

[8] O. Eyercioglu, M. Aladag, S. Sever, Temperature evaluation and bonding quality of large scale additive manufacturing thin wall parts, Sigma J Eng Nat Sci. 36 (2018) 645–654.

[9] W. Zhong, F. Li, Z. Zhang, L. Song, Z. Li, Short fiber reinforced composites for fused deposition modeling, Mater. Sci. Eng. A. 301 (2001) 125–130. https://doi.org/10.1016/S0921-5093(00)01810-4.

[10] R.T.L. Ferreira, I.C. Amatte, T.A. Dutra, D. Bürger, Experimental characterization and micrography of 3D printed PLA and PLA reinforced with short carbon fibers, Compos. Part B Eng. 124 (2017) 88–100. https://doi.org/10.1016/j.compositesb.2017.05.013.

[11] C. Duty, J. Failla, S. Kim, T. Smith, J. Lindahl, V. Kunc, Z-Pinning approach for 3D printing mechanically isotropic materials, Addit. Manuf. 27 (2019) 175–184. https://doi.org/10.1016/j.addma.2019.03.007.

[12] B.N. Turner, R.J. Strong, S. Gold, A review of melt extrusion additive manufacturing processes: I. Process design and modeling, Rapid Prototyp. J. 20 (2014) 192–204.

[13] J.F. Rodríguez, J.P. Thomas, J.E. Renaud, Mechanical behavior of acrylonitrile butadiene styrene (ABS) fused deposition materials. Experimental investigation, Rapid Prototyp. J. 7 (2001) 148–158. https://doi.org/10.1108/13552540110395547.
[14] Q. Sun, G.M. Rizvi, C.T. Bellehumeur, P. Gu, Effect of processing conditions on the bonding quality of FDM polymer filaments, Rapid Prototyp. J. 14 (2008) 72–80. https://doi.org/10.1108/13552540810862028.
[15] S.C. Partain, Fused deposition modeling with localized pre-deposition heating using forced air, Thesis, Montana State University - Bozeman, College of Engineering, 2007. https://scholarworks.montana.edu/xmlui/handle/1/2016 (accessed September 1, 2021).
[16] A.K. Ravi, A. Deshpande, K.H. Hsu, An in-process laser localized pre-deposition heating approach to inter-layer bond strengthening in extrusion based polymer additive manufacturing, J. Manuf. Process. 24 (2016) 179–185. https://doi.org/10.1016/j.jmapro.2016.08.007.
[17] A. Kurapatti Ravi, A Study on an In-Process Laser Localized Pre-Deposition Heating Approach to Reducing FDM Part Anisotropy, M.S., Arizona State University, n.d. https://www.proquest.com/docview/1829549537/abstract/E227499866614B3APQ/1 (accessed September 1, 2021).
[18] V. Kishore, C. Ajinjeru, A. Nycz, B. Post, J. Lindahl, V. Kunc, C. Duty, Infrared preheating to improve interlayer strength of big area additive manufacturing (BAAM) components, Addit. Manuf. 14 (2017) 7–12. https://doi.org/10.1016/j.addma.2016.11.008.
[19] C.E. Duty, J.A. (ORCID:0000000175271647) Failla, S. (ORCID:0000000250312585) Kim, J.M. (ORCID:0000000346350789) Lindahl, B.K. (ORCID:0000000214502250) Post, L.J. (ORCID:0000000259347135) Love, V. (ORCID:0000000344057917) Kunc, Reducing mechanical anisotropy in extrusion-based printed parts, Oak Ridge National Lab. (ORNL), Oak Ridge, TN (United States), 2017. https://www.osti.gov/biblio/1474689 (accessed September 2, 2021).
[20] C.E. Duty, K. Seokpum, K. Vlastimil, L.J. Love, B.K. Post, J.A. Failla, J.M. Lindahl, Z-AXIS IMPROVEMENT IN ADDITIVE MANUFACTURING, n.d. https://appft.uspto.gov/netacgi/nph-Parser?Sect1=PTO2&Sect2=HITOFF&u=%2Fnetahtml%2FPTO%2Fsearch-adv.html&r=1&p=1&f=G&l=50&d=PG01&S1=62491313&OS=62491313&RS=62491313.
[21] A.P. Mouritz, Review of z-pinned composite laminates, Compos. Part Appl. Sci. Manuf. 38 (2007) 2383–2397. https://doi.org/10.1016/j.compositesa.2007.08.016.
[22] A.P. Mouritz, M.K. Bannister, P.J. Falzon, K.H. Leong, Review of applications for advanced three-dimensional fibre textile composites, Compos. Part Appl. Sci. Manuf. 30 (1999) 1445–1461. https://doi.org/10.1016/S1359-835X(99)00034-2.
[23] C. Duty, J. Failla, S. Kim, T. Smith, J. Lindahl, A. Roschli, B. Post, L. Love, V. Kunc, Z-Pinning Approach for Reducing Mechanical Anisotropy of 3D Printed Parts, (n.d.) 8.
[24] DXTech, Technical Data & Safety Specifications: CarbonX CF-PLA 3D Printing Filament, SDS Rev 3.0 - 3DXTECH, (n.d.). https://www.3dxtech.com/tech-data-sheets-safety-data-sheets/ (accessed September 1, 2021).
[25] Internal Thermogravimetric Analysis (TGA) Report, n.d.
[26] ASTM D638 - Tensile, Google Docs. (n.d.). https://docs.google.com/document/u/1/d/1bT-0cKG1DXGgBSmAOD1uPM1q1wozosJcFa9f01hXN0Q/edit?usp=drive_web&ouid=105832583513742308009&usp=embed_facebook (accessed September 2, 2021).

[27] S. Kim, T. Smith, J. Condon, A. Lambert, V. Kunc, C. Duty, GEOMETRIC PARAMETER ANALYSIS OF VERTICALLY EXTRUDED PINS FOR STRENGTH IMPROVEMENT IN ADDITIVE MANUFACTURING WITH FIBER-REINFORCED THERMOPLASTIC, (n.d.) 11.